ACS OMEGA

http://pubs.acs.org/journal/acsodf

Article

Preparation and Characterization of Aprepitant Solid Dispersion with HPMCAS-LF

Jinwen Liu, Yongji Li, Wuliji Ao, Yingge Xiao, Meirong Bai, and Shuyan Li*

Cite This: *ACS Omega* 2022, 7, 39907−39912

Read Online

ACCESS | Metrics & More | Article Recommendations

ABSTRACT: This study focused on improving the physicochemical characteristics of aprepitant with poor water solubility by preparing solid dispersion (SD). To prepare the SD with HPMCAS-LF, the solvent evaporation method was applied. Based on dissolution analysis, the dissolution rate of SD increased by five times compared with aprepitant. In addition, scanning electron microscopy (SEM), X-ray powder diffraction (XRPD), and differential scanning calorimetry (DSC) results suggested the presence of amorphous-form aprepitant inside SD. According to Fourier transform infrared (FTIR) spectroscopy, intermolecular hydrogen bonds were detected between polymer and aprepitant. The Caco-2 cell experiment proved that SD did not lower the transepithelial electrical resistance (TEER) values but improved the permeation amount of aprepitant. Additionally, the SD of aprepitant displayed excellent stability.

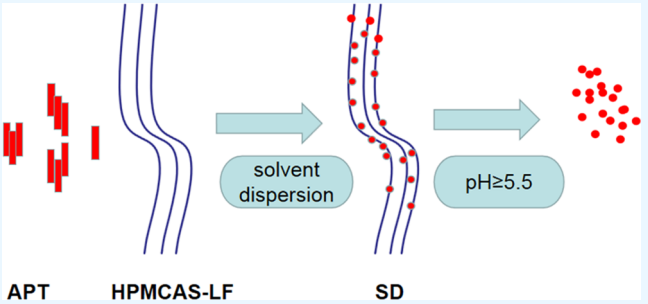

1. INTRODUCTION

Aprepitant is the nonpeptide antagonist of neurokinin 1(NK1). The Food and Drug Association (FDA) approved the application of aprepitant to prevent chemotherapy-induced nausea and vomiting (CINV) over a decade ago. Aprepitant, the selective human substance P/NK1 receptor antagonist, shows high affinity and serves as the therapeutic target for CINV, vomiting, and nausea after surgery.[1−4] Aprepitant is the fundamental compound, whose pKa value is 9.7 and the pH value is 2−12. Within the pH range of 2−10, it has extremely low solubility in free base solution (3−7 μg/mL).[5,6] Aprepitant cannot be applied as a systemic and effective therapy using conventional formulations due to its low solubility.[7] The existing aprepitant formulation in the market is developed by nanoparticle (NP) technology, where drug NPs increase solubility. Nevertheless, NP technology has a complicated processing process; as a result, it is necessary to investigate an alternative technique to improve the solubility.[8,9]

Some technologies may be adopted for enhancing the bioavailability and dissolution of drugs with low water solubility, including surfactant use, size and particle size decrease,[10,11] complexation of cyclodextrin inclusions, formation of salts,[12,13] solid dispersion,[14−17] adjustment of pH value, emulsions,[18] and application of drugs or prodrugs in the lipid or polymeric formulations.[19] According to the specific drug physicochemical properties, most of the above methods are utilized.[20]

Solid dispersions are considered one of the most efficient methods, involving the mixture of a poorly water−soluble drug in one or more hydrophilic carriers in the solid state.[21,22] In solid dispersion systems, a hydrophobic, poorly soluble drug is molecularly dispersed in a hydrophilic polymeric matrix to alter the crystalline state of the drug to an amorphous state, which effectively improves its solubility and dissolution rate. Two methods are mainly proposed for preparing solid dispersions: the melting method and the solvent evaporation method.[23,24] In the hot melt extrusion method, solid dispersions can be prepared by melting the drug within a carrier, cooling the mixture, and pulverizing the final product. The drug and the carrier can be dissolved in a volatile solvent in the solvent evaporation method. Subsequently, the solvent can be evaporated using a vacuum or an oven. In the end, the resulting film is pulverized.[25,26]

Hypromellose methylcellulose acetate succinate (HPMCAS) is usually applied as a coating material for enteric products or as a skeleton material for sustained-release formulations. HPMCAS features an amphiphilic property since it consists of acetic acid and succinic acid esters of hydroxypropyl methyl cellulose. There are three types of HPMCAS on the market, HPMCAS-LF, HPMCAS-MF, and HPMCAS-HF, which are categorized by the varying ratio of acetyl and succinyl groups in the polymer. Different types of HPMCAS have various

Received: July 2, 2022
Accepted: October 13, 2022
Published: October 24, 2022

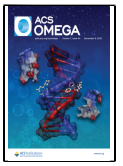

interactions with drugs and prefer to dissolve at varying pH.[27−29] Because of the varying contents of acetyl and succinyl groups of the polymer, the LF, MF, and HF types dissolve at pH 5.5, 6.0, and 6.8, respectively. Moreover, it is described that various kinds of solid dispersion have been prepared with HPMCAS because it can highly hinder the crystallization of drugs in supersaturated solutions.[30,31]

Therefore, this study focused on preparing the solid dispersion (SD) for aprepitant to maximally increase its oral bioavailability and dissolution using the least carrier amount. Specifically, an in-depth evaluation of the binary SD of APT with Soluplus (an amphiphilic copolymer) was recently performed by several different research groups.[32,33] Aprepitant is absorbed in the intestine.[34−36] The preparation of aprepitant solid dispersions using enteric-soluble materials as carriers has not been reported. An amphiphilic polymer LF was explored as the carrier to prepare SD. The prepared SD was characterized according to saturation dissolution, stability, X-ray powder diffraction (XRPD), Fourier transform infrared (FTIR) spectroscopy, scanning electron microscopy (SEM), and differential scanning calorimeter (DSC).

2. MODELS AND METHODS

2.1. Materials. Aprepitant (purity, 99%) was provided by Wuhan Kailun Chemical & Advanced Materials Co., Ltd. (China). HPMCAS-LF was obtained from Shin-Etsu Chemical Co., Ltd. (Japan). The analytically pure acetone and chromatographically pure acetonitrile were provided by Yuwang Industrial Co., Ltd (China). In the current experiment, deionized water (DW) was utilized. The remaining chemicals were analytically pure.

2.2. SD Preparation. This study prepared SD for aprepitant using HPMCAF-LF by solvent evaporation. Briefly, aprepitant was mixed with HPMCAS-LF (weight ratios of drug/HPMCAS-LF, 1:3, 1:4, 1:5) in 10 mL of acetone. Subsequently, we heated the mixture to evaporate the solvent under constant stirring. The solution was stirred at 100 rpm, and the temperature was held at 70 °C. Later, SD was preserved overnight under vacuum. Afterward, a pestle and mortar were utilized to grind the mixture. Next, the mixture was filtered with the 50-mesh sieve. Thereafter, the resultant products were preserved within a desiccator for subsequent analysis.

2.3. Dissolution Study. A dissolution study was performed in line with the Chinese Pharmacopeia (2015 ED) Method II. Therefore, the current work utilized the ZRS-8L dissolution equipment (Tianda Tianfa, China) using the paddle approach. SD equating with 25 mg of pure aprepitant was positioned in PBS 6.6 (250 mL) that contained 0.1% sodium dodecyl sulfate under stirring at 50 rpm and 37 ± 0.5 °C. Later, a 0.6 mL sample was gathered at the predetermined time points, and an equivalent medium was added to maintain an unchanged volume. Thereafter, the collected sample was filtered with a 0.45 μm membrane filter. In addition, the approved HPLC approach was utilized to determine the dissolved drug amounts at specific time points.

The HPLC system, which consisted of an SPD-10A VP UV detector and an LC-10A VP pump (Shimadzu, Japan), was adopted for analysis. The Phenomenex C8 column (150 × 4.6 mm^2, 5 μm) was utilized to separate the sample. The mobile phase consisted of acetonitrile and 0.05% phosphate (40:40, v/v), with the flow rate being 1.0 mL/min. In addition, the column temperature and the UV detector were 30 °C and 210 nm, respectively.

2.4. Differential Scanning Calorimetry (DSC). We adopted a differential scanning calorimeter (DSC-1, Mettler, USA) for adopting thermograms for SD, aprepitant, and physical mixtures. Thereafter, an approximately 3 mg sample was collected, examined within pierced Al crucibles, and heated from 30 to 300 °C at a 10 °C/min heating rate in a nitrogen atmosphere.

2.5. X-ray Powder Diffraction (XRPD) Analysis. This study employed a universal diffractometer (X′Pert PRO, PANalytical, Holland) for XRPD analysis, with Cu Kα monochromatic radiation (λ = 1.540598 Å). X-ray in the anode tube ran at 40 mA and 40 kV. Thereafter, the sample was placed into the aluminum sample port; then, X-ray deflection was detected within the range of 5−60°, and the size was set at 0.01670° 2θ.

2.6. Fourier Transform Infrared (FTIR) Spectroscopy. An infrared spectrophotometer (EQUINOX55, Bruker, Germany) was adopted for FTIR analysis at ambient temperature. To this end, in this study, we ground HPMCAS-LF, aprepitant, SD, and PM samples and blended them sufficiently using potassium bromide before any measurement. The following parameters were set: resolution, 1 cm^{-1} and scanning range, 400−4000 cm^{-1}.

2.7. Scanning Electron Microscopy (SEM). To observe SD and PM morphologies, a scanning electron microscope (Inspect50, FEI, USA) was applied. First, a vacuum evaporator was utilized to coat samples with palladium and gold. Subsequently, samples were explored at a 10 kV accelerating voltage.

2.8. In Vitro Permeation Tests. Caco-2 cells were provided by ATCC (USA) as the model gastrointestinal epithelial cells; cultured with DMEM consisting of 10% fetal bovine serum (FBS, after heat inactivation), 1% nonessential amino acids, and 0.1% gentamicin; and then incubated with a humid incubator under 5% CO_2 and 37 °C conditions. Thereafter, cells were collected at passages 60−80 and inoculated (4.5 × 105/cm^2) onto the polycarbonate filter inserts (area, 4.9 cm^2; pore size, 2 cm; Trans well, Coning, NY). Later, cells were cultured for 23−28 days within the medium prior to permeation tests. Thereafter, a Millicell-ERS (Millipore, MA) was adopted for measuring transepithelial electrical resistances (TEERs) to assess the quality of the monolayer grown on permeable membranes. In this study, the TEER value was ≥350 Ω/cm^2.

Aprepitant (10 mg), SD, and Emend (10 mg as aprepitant) were mixed into 1 mL of PBS that contained 0.5% CMC-Na (pH 7.4). Thereafter, 300 μL of suspension was immediately added to the upper surface of Caco-2 cell monolayers. Later, 600 μL of DMEM (pH 7.4) was treated as the basolateral side solution and replaced every 30 min for 2 h. Additionally, TEER pre- and postpermeation tests were conducted according to a previous description. HPLC analysis was adopted for determining aprepitant contents with the basolateral side solution according to the previous description. Results were displayed in the form of permeated aprepitant amount. Then, the permeation rate was divided by saturated solubility within the suspension used for Caco-2 cell monolayers, aiming to determine the apparent permeation clearance.

2.9. Stability Test. The as-prepared SD was preserved within an artificial climate box under 60% relative humidity

https://doi.org/10.1021/acsomega.2c04021
ACS Omega 2022, 7, 39907−39912

(RH) and 40 °C conditions for 6 months. Then, the dissolution degree was detected in 0, 1, 3, and 6 months.

3. RESULTS AND DISCUSSION

3.1. Dissolution Study. Figure 1 compares the diverse aprepitant SD release rates in pure drug and PBS (pH 6.6),

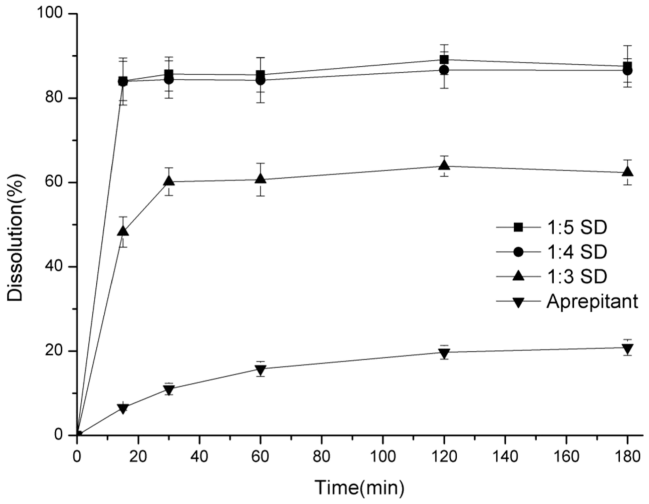

Figure 1. Aprepitant and SD dissolution profiles under diverse aprepitant/HPMCAS-LF ratios (1:5, 1:4, 1:3). All points stand for mean ± SD (n = 3).

including 0.1% SDS. Obviously, each SD increased the aprepitant dissolution rate, conforming to the increased drug solubility in such formulations. The pure drug showed poor dissolution, and the release rate was 11.02 ± 1.36% in 30 min and 20.87 ± 1.88% in 180 min. Moreover, there was a distinct trend between aprepitant dissolution and LF ratios as expected. The release rate of 1:5 SD formulation was 86.69 ± 5.03% within 30 min, suggesting that the drug dissolution increased by eight times during this period. By contrast, the release rates of 1:4 and 1:5 SD formulations were 87.51 ± 4.19 and 86.69 ± 5.03%, respectively, and they displayed greater dissolution rates and close release curves compared with those of 1:3 SD formulations. Faster dissolution of aprepitant in solid dispersions might be explained by improved drug wetting in the dissolution medium and the conversion of the drug from crystalline to the amorphous state. The drug was already amorphous in 1:4 SD; therefore, 1:4 and 1:5 SD had similar dissolution rates. Therefore, this study selected the 1:4 SD formulation for subsequent analysis.

3.2. DSC. Figure 2 presents the thermal behaviors of HPMCAS-LF, pure aprepitant, SD, and physical mixtures. Clearly, the melting endothermic peak of the pure drug was detected at 253.2 °C, which was not found in SD, suggesting that aprepitant had no melting endotherm. The peak position of physical mixing was shifted, suggesting that the drug and excipients interact at high temperatures. Based on the above results, aprepitant existed in the amorphous form in the as-prepared SD.

3.3. XRPD. XRPD images for aprepitant, HPMCAS-LF, SD, and physical mixtures can be observed in Figure 3. The pure drug showed intense and sharp peaks within the 2θ = 5−60° range, suggesting the presence of aprepitant in the crystalline state. For aprepitant, its main typical crystalline peaks were distinctly detected within the PM diffractograms. However, its

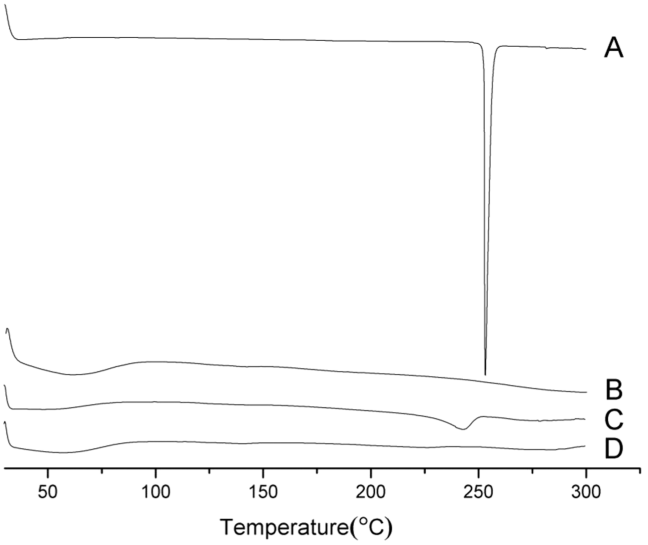

Figure 2. DSC curves for (A) aprepitant, (B) HPMCAS-LF, (C) 1:4 physical mixture, and (D) SD.

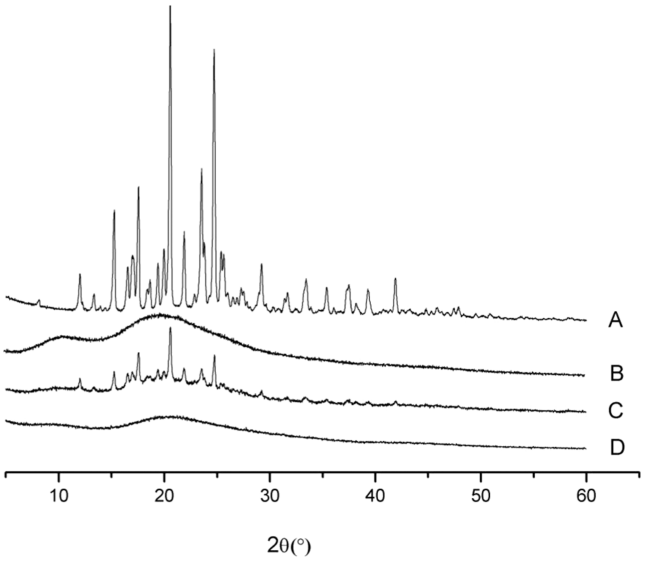

Figure 3. XRPD spectra for (A) aprepitant, (B) HPMCAS-LF, (C) 1:4 physical mixture, and (D) 1:4 SD.

discriminatory peaks disappeared in SDs (1:4), suggesting the existence of aprepitant in the amorphous form, which was in consistence with DSC findings.

3.4. FTIR Spectroscopy. FTIR spectroscopy is extensively adopted for investigating the potential drug−polymer interactions within the SD systems. To assess the potential solid−solid interactions between carriers and the drug, the FTIR spectra for aprepitant, SD, and physical mixtures were obtained, as presented in Figure 4a,b.

From the FTIR spectra of aprepitant, typical peaks were detected at 1704, 1132, and 1500−1600 cm^{-1}, respectively, caused by C═O, C−F, and C−H stretching. LF spectra revealed that peaks were detected at 1740 and 1641 cm^{-1}, which resulted from C═O stretching. Meanwhile, an OH peak was also detected at 3447 cm^{-1}. Aprepitant, physical mixtures, and HPMCAS-LF showed similar FTIR spectra to aprepitant and HPMCAS-LF.

https://doi.org/10.1021/acsomega.2c04021
ACS Omega 2022, 7, 39907−39912

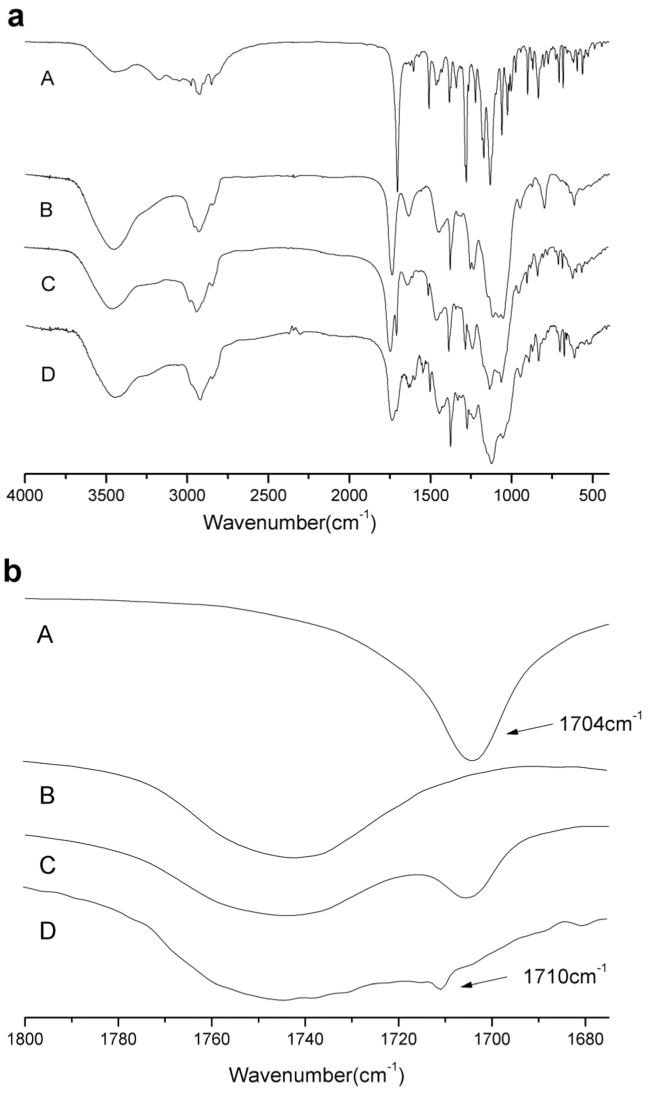

Figure 4. FTIR spectra of (A) aprepitant, (B) HPMCAS-LF, (C) 1:4 physical mixture, and (D) 1:4 SD.

For SD (1:4) formulation, a weak peak was detected at 3444 cm^{-1} on the spectrum, which was attributed to the −OH stretching vibration. At the same time, the peak of SD shifted from 1704 cm^{-1} (C═O) (crystal drug) to 1710 cm^{-1}. The above results indicated the interaction between aprepitant and HPMCAS-LF, probably due to the hydrogen bonding.

3.5. SEM. SEM was conducted to examine PM and SD morphologies. Figure 5 shows the photographs. Obviously, aprepitant powders were platelike crystals that had smooth surfaces. However, SD were particles with an irregular shape. On the contrary, aprepitant did not show any crystal structure within SD, which indicated that aprepitant transformed to the amorphous state, conforming to DSC and XRPD results.

3.6. In Vitro Permeation Experiments. The amounts of aprepitant permeating via the Caco-2 cell monolayers using aprepitant, Emend, and 1:4 SD are presented in Figure 6. The permeated amount of aprepitant increased after aprepitant addition at all time points. Amorphous aprepitant had higher solubility and dissolution rate, which therefore made it easier for it to pass through the Caco-2 membrane. However, the superior permeating amount of Emend (an aprepitant commercial capsule) was interpreted from the effects below. Initially, smaller drug particles with greater surface area and lower thickness of the diffusion layer might be quickly absorbed via the gastrointestinal wall. Second, there were surfactants within the formulations, enhancing aprepitant absorption and dissolution into the gastrointestinal tract.[31] For the Caco-2 cell monolayers, their TEER values pre- and postpermeation tests can be found in Figure 7. Therefore, there existed no significant differences in TEER after permeation experiments.

3.7. Stability Study. As shown in Figure 8, the long-term stability of the aprepitant SD was studied. After 6 months, differences in dissolution rate were not statistically significant among the three samples, namely, pure drug, 1:4 SD, and 1:5 SD formulations, indicating the amorphous status of aprepitant in the latter two formulations. The dissolution rate of 1:3 SD was significantly reduced by 42.4 ± 3.5% within 30 min, and that for 1:4 SD was 82.5 ± 4.3%. Therefore, it was concluded that a specific aprepitant/HPMCAS-LF ratio must be acquired to obtain stable SD.

4. CONCLUSIONS

To conclude, this study prepared and analyzed aprepitant SD using HPMCAS-LF. According to our results, SD technology markedly enhanced the aprepitant dissolution rate. FTIR spectroscopy showed that there were intermolecular hydrogen bonds between LF and aprepitant. Additionally, DSC, XRPD, and SEM results suggested that the drug existed in an amorphous state in SD. HPMCAS-LF did not reduce the Caco-2 TEER values, whereas HPMCAS-LF increased the amount of aprepitant in Caco-2 cells. In addition, the SD of aprepitant had excellent stability.

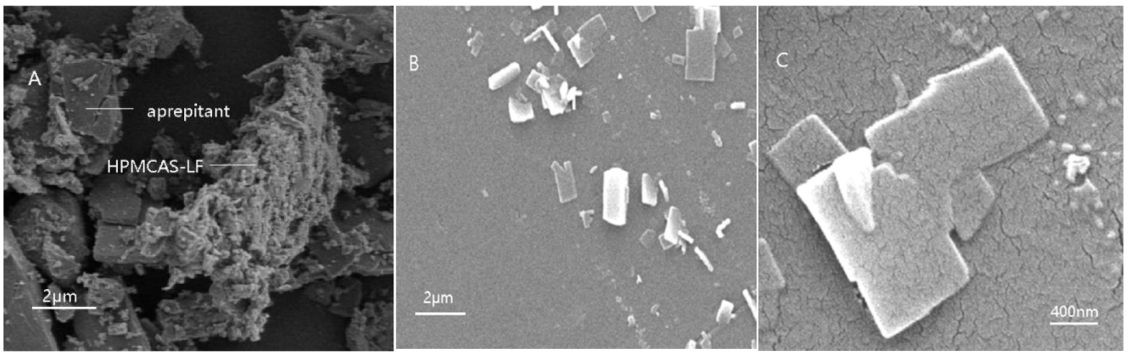

Figure 5. SEM photomicrographs of 1:4 PM (A), 1:4 SD (10000X) (B), and 1:4 SD (50000X) (C).

https://doi.org/10.1021/acsomega.2c04021
ACS Omega 2022, 7, 39907−39912

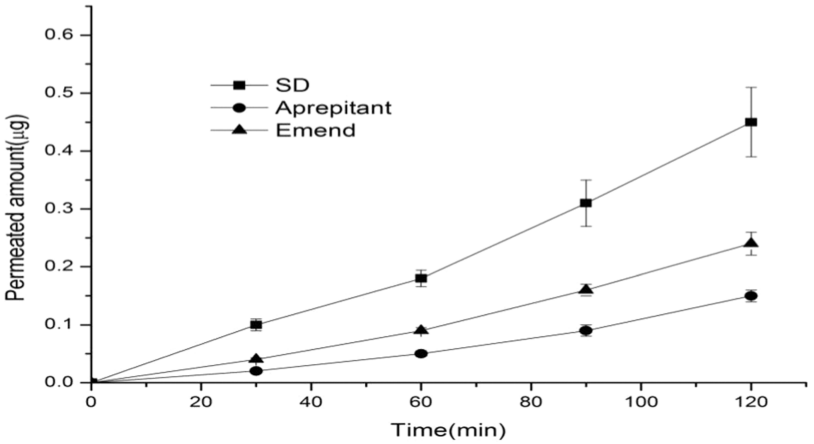

Figure 6. Amount of aprepitant permeated through Caco-2 cells.

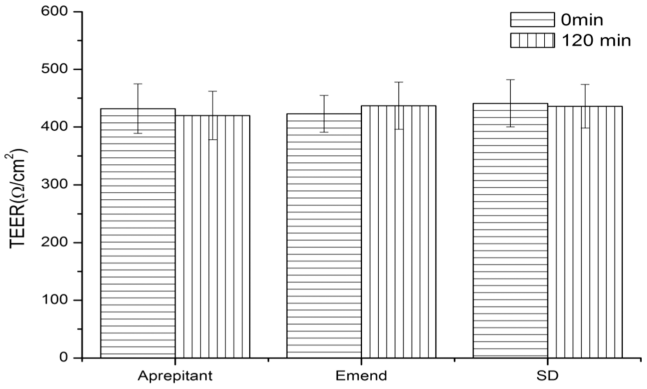

Figure 7. TEER values for the Caco-2 cells pre- and postpermeation tests.

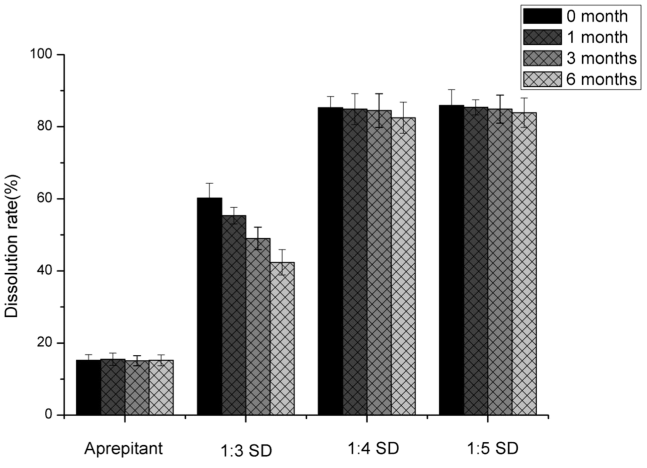

Figure 8. Aprepitant dissolution rate of diverse samples within 30 min.

AUTHOR INFORMATION

Corresponding Author

Shuyan Li − *College of Traditional Mongolian Medicine, Inner Mongolia Minzu University, Tongliao 028000, China;* Email: lishuyan@imun.edu.cn

Authors

Jinwen Liu − *College of Traditional Mongolian Medicine, Inner Mongolia Minzu University, Tongliao 028000, China;*

School of Pharmacy, Heilongjiang University of Traditional Chinese Medicine, Harbin 150040, China; orcid.org/0000-0002-2539-3731

Yongji Li − *School of Pharmacy, Heilongjiang University of Traditional Chinese Medicine, Harbin 150040, China*

Wuliji Ao − *Inner Mongolia Research Institute of Traditional Mongolian Meweight ratios ofdicine Engineering, Tongliao 028000, China*

Yingge Xiao − *College of Traditional Mongolian Medicine, Inner Mongolia Minzu University, Tongliao 028000, China*

Meirong Bai − *Key Laboratory of Monglian Medicine Research and Development Engineering, Ministry of Education, Tongliao 028000, china*

Complete contact information is available at: https://pubs.acs.org/10.1021/acsomega.2c04021

Author Contributions

J.L., W.A., and M.B. designed the experiment; S.L., Y.L., and Y.X. carried out the experiment; and J.L. wrote the manuscript.

Funding

The study was funded by the "Innovation Team Development Plan" Project of Inner Mongolia colleges and universities (NMGIRT2216), Interdisciplinary construction projects supported by special funds for local construction from the central government (JCHXKXM001), Mongolian Medicine Safety evaluation innovation team project (MY20190003), Mongolian Medicine Standardization project of Inner Mongolia People's Government (2021MB028), Natural Science Foundation of Inner Mongolia (2021MS08074), Inner Mongolia science and technology planning project (2021GG0428), and the "Young Science and Technology Talents Support Program" of Inner Mongolia Colleges and Universities (NJYT22049).

Notes

The authors declare no competing financial interest.

REFERENCES

(1) Sorbera, L. A.; Castañer, J.; Bayés, M.; Silvestre, J. Aprepitant and L-758298. *Drugs Future* **2002**, *27*, 211−222.

(2) Nama, S.; Chandu, B. R.; Awen, B. Z.; Khagga, M. Development and Validation of a New RP-HPLC Method for the Determination of Aprepitant in Solid Dosage Forms. *Trop. J. Pharm. Res.* **2011**, *10*, 491−497.

(3) Cocquyt, V.; Van Belle, S.; Belle, S. V.; Reinhardt, R. R.; Decramer, M.; O'Brien, M.; O'Brien, M.; Schellens, J.; Schelle, J. H.;

https://doi.org/10.1021/acsomega.2c04021
ACS Omega 2022, 7, 39907−39912

Borms, M.; Verbeke, L.; Verbeke, L.; Van, A. F.; Van Aelst, F.; De, S. M.; De Smet, M.; Carides, A. D.; Carides, A.; Eldridge, K.; Eldridge, K.; Gretz, B. J. Comparison of L-758,298, a prodrug for the selective neurokinin-1 antagonist, L-754,030, with ondansetron for the prevention of cisplatin-induced emesis. *Eur. J. Cancer.* **2001**, *37*, 835−842.

(4) Wu, Y.; Loper, A.; Landis, E.; Hettrick, L.; Novak, L.; Lynn, K.; Chen, C.; Thompson, K.; Higgins, R.; Batra, U.; Shelukar, S.; Kwei, G.; Storey, D. The role of biopharmaceutics in the development of a clinical nanoparticle formulation of MK-0869: a Beagle dog model predicts improved bioavailability and diminished food effect on absorption in human. *Int. J. Pharm.* **2004**, *285*, 135−146.

(5) Rosso, M.; et al. The Role of Neurokinin-1 Receptor in the Microenvironment of Inflammation and Cancer. *Sci. World. J.* **2012**, *4*, No. 381434.

(6) Olver, I.; Shelukar, S.; Thompson, K. C. Nanomedicines in the treatment of emesis during chemotherapy: focus on aprepitant. *Int. J. Nanomed.* **2007**, *2*, 13−18.

(7) Ren, L.; Zhou, Y.; Wei, P.; Li, M.; Chen, G. Preparation and pharmacokinetic study of aprepitant-sulfobutyl ether-β-cyclodextrin complex. *AAPS PharmSciTech* **2014**, *15*, 121−130.

(8) Singare, D. S.; Marella, S.; Gowthamrajan, K.; Kulkami, G. T.; Vooturi, R.; Rao, P. S. Optimization of formulation and process variable of nanosuspension: An industrial perspective. *Int. J. Pharm.* **2010**, *402*, 213−220.

(9) Ridhurkar, D. N.; Ansari, K. A.; Kumar, D.; Kaul, N. S.; Krishnamurthy, T.; Dhawan, S.; Pillai, R. Inclusion complex of aprepitant with cyclodextrin: evaluation of physico-chemical and pharmacokinetic properties. *Drug Dev. Ind. Pharm.* **2013**, *39*, 1783−1792.

(10) Müller, R. H.; Jacobs, C.; Kayser, O. Nanosuspensions as particulate drug formulations in therapy:Rationale for development and what we can expect for the future. *Adv. Drug Delivery Rev.* **2001**, *47*, 3−19.

(11) Basa, S.; Muniyappan, T.; Karatgi, P.; Prabhu, R.; Pillai, R. Production and in vitro characterization of solid dosage form incorporating drug nanoparticles. *Drug Dev. Ind. Pharm.* **2008**, *34*, 1209−1218.

(12) Humberstone, A. J.; Charman, W. N. Lipid-based vehicles for the oral delivery of poorly water soluble drugs. *Adv. Drug Delivery Rev.* **1997**, *25*, 103−128.

(13) Pouton, C. W. Lipid formulations for oral administration of drugs: non-emulsifying, self-emulsifying and 'self-microemulsifying' drug delivery systems. *Eur. J. Pharm Sci.* **2000**, *11*, S93−S98.

(14) Wang, X.; Li, L.; Huo, W.; Hou, L.; Zhao, Z.; Li, W. Characterization and Stability of Tanshinone IIA Solid Dispersions with Hydroxyapatite. *Materials* **2013**, *6*, 805−816.

(15) Linn, M.; Collnot, E. M.; Djuric, D.; Hempel, K.; Fabian, E.; Kolter, K.; Lehr, C. M. Soluplus as an effective absorption enhancer of poorly soluble drugs in vitro and in vivo. *Eur. J. Pharm. Sci.* **2012**, *45*, 336−343.

(16) Eloy, J. O.; Marchetti, J. M. Solid dispersions containing ursolic acid in Poloxamer 407 and PEG 6000: A comparative study of fusion and solvent methods. *Powder Technol.* **2014**, *253*, 98−106.

(17) Maali, A.; Hamed Mosavian, M. T. Preparation and Application of nanoemulsions in the last decade (2000−2010). *J. Dispersion Sci. Technol.* **2013**, *34*, 92−105.

(18) Maulvi, F. A.; Dalwadi, S. J.; Thakkar, V. T.; Soni, T. G.; Gohel, M. C.; Gandhi, T. R. Improvement of dissolution rate of aceclofenac by solid dispersion technique. *Powder Technol.* **2011**, *207*, 47−54.

(19) Guo, Z.; Boyce, C.; Rhodes, T.; Liu, L.; Leung, D. H.; et al. A novel method for preparing stabilized amorphous solid dispersion drug formulations using acoustic fusion. *Int. J. Pharm.* **2021**, *592*, No. 120026.

(20) Streubel, A.; Siepmann, J.; Peppas, N. A.; Bodmeier, R. Bimodal drug release achieved with multi-layer matrix tablets: transport mechanisms and device design. *J. Controlled Release* **2000**, *69*, 455−468.

(21) Chandrasekhara Rao, B.; et al. Dissolution enhancement of poorly soluble drug aprepitant by hot melt extrusion method using hydrophilic polymer: A solid dispersion technique. *Res. J. Pharm. Biol. Chem. Sci.* **2014**, *5*, 1469−1485.

(22) Adil, V.; Rajput, D.; Jain, S.; Kapoor, V.; Gupta, N. Formulation and development of lamotrigine fast dissolving tablet by enhancing its solubility through solid dispersion. *Res. J. Pharm. Technol.* **2021**, *14*, 873−878.

(23) Poudel, S.; Dong, W. K. Developing pH-Modulated Spray Dried Amorphous Solid Dispersion of Candesartan Cilexetil with Enhanced In Vitro and In Vivo Performance. *Pharmaceutics* **2021**, *13*, 497.

(24) Alkufi, H. K.; Rashid, A. M. Enhancement of the solubility of famotidine solid dispersion using natural polymer by solvent evaporation. *Int. J. App. Pharm.* **2021**, *13*, 193−198.

(25) Paradkar, A.; Ambike, A. A.; Jadhav, B. K.; Mahadik, K. R. Characterization of curcumin-PVP solid dispersion obtained by spray drying. *Int. J. Pharm.* **2004**, *271*, 281−286.

(26) Lakshman, J. P.; Cao, Y.; Kowalski, J.; Serajuddin, A. Application of melt extrusion in the development of a physically and chemically stable high-energy amorphous solid dispersion of a poorly water-soluble drug. *Mol. Pharmaceutics* **2008**, *5*, 994−1002.

(27) Zhang, Q.; Zhao, Y.; Zhuang, Y.; Ding, Z.; Fan, Z.; et al. Effect of HPMCAS on recrystallization inhibition of nimodipine solid dispersions prepared by hot-melt extrusion and dissolution enhancement of nimodipine tablets. *Colloids Surf., B* **2018**, *172*, 118−1206.

(28) Zhao, Y.; Xin, T.; Ye, T.; Yang, X.; Pan, W. Solid dispersion in the development of a nimodipine delayed-release tablet formulation. *Asian. J. Pharm. Sci.* **2014**, *9*, 2100−2110.

(29) Li, B.; Konecke, S.; Wegiel, L. A.; Taylor, L. S.; Edgar, K. J. Both solubility and chemical stability of curcumin are enhanced by solid dispersion in cellulose derivative matrices. *Carbohydr. Polym.* **2013**, *98*, 1108−1116.

(30) Honick, M.; Das, S.; Hoag, S. W.; Muller, F. X.; Polli, J. E.; et al. The effects of spray drying, HPMCAS grade, and compression speed on the compaction properties of itraconazole-HPMCAS spray dried dispersions. *Eur. J. Pharm. Sci.* **2020**, *155*, No. 105556.

(31) Jachowicz, R.; Czech, A. Preparation and evaluation of piroxicam-HPMCAS solid dispersions for ocular use. *Pharm. Dev. Technol.* **2008**, *13*, 495−504.

(32) Liu, J.; Zou, M.; Piao, H.; Liu, Y.; Tang, B.; Gao, Y.; Ma, N.; Cheng, G. Characterization and Pharmacokinetic Study of Aprepitant Solid Dispersions with Soluplus. *Molecules* **2015**, *20*, 11345−11356.

(33) Nanaki, S.; Eleftheriou, R. M.; Barmpalexis, P.; Kostoglou, M.; Karavas, E.; Bikiaris, D. Evaluation of Dissolution Enhancement of Aprepitant Drug in Ternary Pharmaceutical Solid Dispersions with Soluplus and Poloxamer 188 Prepared by Melt Mixing. *Sci* **2019**, *1*, 48.

(34) Shono, Y.; Jantratid, E.; Kesisoglou, F.; Reppas, C.; Dressman, J. B. Forecasting in vivo oral absorption and food effect of micronized and nanosized aprepitant formulations in humans. *Eur. J. Pharm. Biopharm.* **2010**, *76*, 95−104.

(35) Litou, C.; Patel, N.; Turner, D. B.; Edmund, K.; Martin, K.; Box, K. J.; Jennifer, D. Combining biorelevant in vitro and in silico tools to simulate and better understand the in vivo performance of a nano-sized formulation of aprepitant in the fasted and fed states. *Eur. J. Pharm. Sci.* **2019**, *138*, No. 105031.

(36) Roos, C.; Dahlgren, D.; Sjögren, E.; Sjöblom, M.; Hedeland, M.; Lennernäs, H. Jejunal absorption of aprepitant from nano-suspensions: Role of particle size, prandial state and mucus layer. *Eur. J. Pharm. Biopharm.* **2018**, *132*, 222−230.

https://doi.org/10.1021/acsomega.2c04021
ACS Omega 2022, 7, 39907−39912